Clim. Past Discuss., 6, 347–368, 2010
www.clim-past-discuss.net/6/347/2010/

Climate
of the Past
Discussions

Surface circulation patterns and the pathways of sea surface carbon dioxide (CO_2) off northern Chile (~27.5° S) between 30 and 10 kyr BP: global and/or local forcing?

J. A. Placencia[1,2,3], **N. Harada**[4], **R. Torres**[5], **C. B. Lange**[2], **and D. Hebbeln**[6]

[1]Graduate Program in Oceanography, Department of Oceanography, University of Concepción, Concepción, Chile

[2]Department of Oceanography and Center for Oceanographic Research in the eastern South Pacific (FONDAP-COPAS), University of Concepción, Concepción, Chile
[3]Department of Environmental Chemistry, Faculty of Sciences, Universidad Católica de la Santísima Concepción, Concepción, Chile
[4]Research Institute for Global Change, Japan Agency for Marine-Earth Science and Technology (JAMSTEC), Yokosuka, Japan
[5]Centro de Investigación en Ecosistemas de la Patagonia (CIEP), Universidad Austral de Chile, Coyhaique, Chile
[6]MARUM Center for Marine Environmental Sciences, Bremen University, Bremen, Germany

Received: 25 February 2010 – Accepted: 1 March 2010 – Published: 31 March 2010

Correspondence to: J. A. Placencia (jplacenc@udec.cl)

Published by Copernicus Publications on behalf of the European Geosciences Union.

Abstract

We present a reconstruction of past changes in partial pressure of CO_2 (pCO_2) from northern Chile (~27° S), between 10 and 30 kyr BP, based on carbon isotope composition of $C_{37:2}$-alkenone. The high-pCO_2 during the entire time series indicates that northern Chile upwelling system has been a permanent source of CO_2 to the atmosphere. The multiproxy reconstruction suggests that the CO_2 outgassing and sequestration pathways were modulated by local and global mechanisms. During global glacial conditions, an enhanced coastal upwelling forcing resulted in high-availability of deep water macronutrients and a CO_2-supersaturated water column, which combined with high-inputs of iron from the continent, intensified the carbon sequestration pathway of the biological pump, through diatom biomass export. During the deglacial, a decrease in the upwelling forcing, an increment in water column stability and reduced continental inputs of iron are consistent with a larger role of calcifying organisms in the plankton assemblage in terms of carbon sequestration pathway through the carbonate system.

1 Introduction

Coastal upwelling areas are often described as intense sources of CO_2 and macronutrients (e.g., Borges et al., 2005). The CO_2-supersaturated and high-macronutrient concentration of upwelled waters stimulate intense blooms of phytoplankton that sequester inorganic carbon thus reducing the outgassing of CO_2 (e.g., Simpson and Zirino, 1980).

Large parts of the ocean have been described as High-Nutrient/Low-Chlorophyll (HNLC) areas, where phytoplankton growth is limited by the availability of iron (e.g., Martin, 1990; de Baar and Boyd, 2000; Bruland et al., 2005). Experimental evidence suggests that the availability of dissolved iron permits the rapid interception of upwelled CO_2 by phytoplankton in oceanic (e.g., Bakker et al., 2001) and coastal waters (Torres and Ampuero, 2009). High-levels of dissolved iron in coastal upwelled waters are determined by the input of iron into the photic layer from other sources (e.g., dust deposition, river discharges, continental shelf) in addition to the initial dissolved iron contained in the water masses that feed the upwelling (Johnson et al., 1999; Bruland et al., 2005).

Upwelling favorable winds are permanent at ∼27° S off Chile during all year (Shaffer et al., 1999). In this area of narrow continental shelf, the recently upwelled water is characterized by low-temperature, high-nutrient concentrations, low-chlorophyll and supersaturation in CO_2 (e.g., Torres et al., 1999; Torres and Ampuero, 2009). At these windy latitudes (27°–30° S) (Shaffer et al., 1999), the supersaturation in CO_2 allows for strong-CO_2 fluxes from the ocean to the atmosphere (e.g., Torres et al., 2002). Vertical fluxes of organic matter and water column stratification are key factors that explain the intensity/extension of aerobic and anaerobic production of CO_2. The intense denitrification reported for upwelling areas off Peru and Chile highlights an additional input of CO_2 associated with anaerobic respiration of organic matter (e.g., Friederich et al., 2008; Paulmier et al., 2008).

Paleoceanographic reconstructions off northern Chile described a strong precessional cyclicity in the pattern of iron flux, suggesting that iron availability is a key factor for past changes in productivity and sequestration of atmospheric CO_2 (Lamy et al., 1998; Dezileau et al., 2004). This was related to increased precipitation during precessional maxima, higher river runoff transporting iron-rich terrigenous material to the ocean inducing high-biological productivity (i.e., diatom blooms) and consequently, a rapid decrease in sea surface water pCO_2 (Dezileau et al., 2004). In contrast, low-precipitation during precessional minima decreased the iron supply to the ocean, thus limiting the primary productivity and enhancing the supersaturation of CO_2 in the surface water column (Dezileau et al., 2004).

Another study suggested that the rapid melting of the most northerly extension of the Patagonian Ice Sheet (Lamy et al., 2004) enhanced water column stratification during the deglacial (De Pol-Holz et al., 2006), which could be translated into reduced physical ventilation of the intermediate water masses (De Pol-Holz et al., 2007).

This study is a first approximation of millennial pCO_2 changes in the eastern South Pacific (ESP) margin between 30 and 10 kyr BP, based on carbon isotope composition of $C_{37:2}$-alkenone. Our results reveal that important changes in the marine CO_2 outgassing were modulated by local and global mechanisms, including water column stability, iron-limitation, and consequently the productivity patterns, which potentially control the different pathways of removal of the marine CO_2 from surface waters to the deep-ocean.

2 Material and methods

We used deep-sea sediment core GeoB 3375-1 (27°28′ S, 71°15′ W; 1947 m water depth; core length 489 cm), collected from the Chilean margin. Sediment samples were sub-sampled at 5 cm, freeze-dried and extracted for alkenone analyses according to the methodology described by Prahl et al. (1988) and Harada et al. (2003).

1–2 grams of freeze-dried sediment was ground into a powder with an agate mortar and pestle. The bulk organic fractions were extracted from sediment samples with an accelerated solvent extractor (ASE-200, Dionex Japan, Ltd.) at 100 °C and 1000 psi using a mixture of dichloromethane and methanol (99:1 v/v) as the solvent. The yield of the extraction procedure was >95% for a ketone standard (2-nonadecanone).

The extracts were saponified in 0.5 M KOH in methanol at 80 °C for 2 h. The neutral fraction was recovered with a pipette, dissolved in hexane, and then separated into subfractions by silica gel column chromatography using an automatic solid preparation system (Rapid Trace SPE Workstation, Zymark, UK). Standards for the subfractionation were hydrocarbons (C_{20}–C_{38} hydrocarbons and 5α-cholestane, GLSciences Inc., Japan), a ketone (2-nonadecanone, Fluka Chemie, Switzerland), and a sterol (cholesterol, GLSciences Inc., Japan). The solvents used were 4 mL of hexane for fraction 1; a mixture of 2 mL of a hexane-toluene mixture (3:1 v/v), 2 mL of hexane-toluene (1:1 v/v), 2 mL of hexane-ethyl acetate (95:5 v/v), and 2 mL of hexane-ethyl acetate (9:1 v/v) for fraction 2; 2 mL of hexane-ethyl acetate (85:15 v/v) followed by 2 mL of hexane-ethyl acetate (4:1 v/v) for fraction 3; and 2 mL of hexane-ethyl acetate (4:1 v/v) followed by 2 mL of ethyl acetate for fraction 4. The alkenones eluted in fraction 3. The recovery of a 2-nonadecanone standard with this procedure was >90%. A sample of the alkenone fraction was analyzed by capillary gas chromatography with a Fisons 8000 series gas chromatograph (CE Instruments, USA) equipped with a 50 m long, 0.32 mm internal diameter Chrompack CP-Sil 5CB fused silica column, a cold on column injector, and a flame ionization detector. The temperature regime for gas chromatography was as follows: held at 60 °C for 1 min, increased to 200 °C at 20 °C min^{-1}, increased to 305 °C at 15 °C min^{-1}, held at 305 °C for 32 min, increased to 320 °C at 15 °C min^{-1}, and held at 320 °C for 5 min.

$U_{37}^{K'}$-index calculations were conducted according to Prahl and Wakeham (1987), and $U_{37}^{K'}$ values were converted to alkenone-based temperature ($U_{37}^{K'}$-SST) using the equation of Prahl et al. (1988), i.e., $U_{37}^{K'}=0.034T+0.039$, where T = temperature (°C).

The $\mathrm{C}_{37:2}$-alkenone isotope analyses were performed using a HP6890 gas chromatography unit and a Finnigan MAT 252 (Thermo Electron Co. Bremen, Germany) mass spectrometer unit. The $^{13}\mathrm{C}/^{12}\mathrm{C}$ isotopic ratio was also measured in a n-C_{36} hydrocarbon (GLSciences Inc., Japan) and National Bureau of Standards standard 19 (International Atomic Energy Agency) as an internal standard. The analytical accuracy of $\delta^{13}\mathrm{C}_{\mathrm{C37:2}}$-alkenone was ±0.05‰.

Alkenone-CO_2 estimates were based on the expression:

$$\varepsilon_{\mathrm{p32:7=}}\varepsilon_f - b/[\mathrm{CO_{2aq}}] \tag{1}$$

where $\varepsilon_{\mathrm{p32:7}}$ values are based on the isotopic difference between an estimate of the $\delta^{13}\mathrm{C}$ values of the organic matter produced by ancient algae ($\delta^{13}\mathrm{C}_{\mathrm{org}}$) and the co-existing dissolved CO_2 in the photic zone ($\delta^{13}\mathrm{C}_{\mathrm{CO2aq}}$) (Freeman and Pagani, 2005). $\delta^{13}\mathrm{C}_{\mathrm{org}}$ is determined by adding 4.2‰ to the measured $\delta^{13}\mathrm{C}_{37:2}$ values, as a correction that reflects lipid-biomass isotopic differences between *Haptophyte* biomass and $\mathrm{C}_{37:2}$-alkenone, with alkenones depleted relative to total organic biomass (e.g., Bidigare et al., 1997; Popp et al., 1998; Pagani et al., 1999). $\delta^{13}C_{CO2aq}$ is reconstructed from the carbon isotope composition of planktic foraminifera, which assumes that isotopic and chemical equilibrium prevailed among all the carbon aqueous species and atmospheric CO_2 as well as foraminiferal calcite (e.g., Pagani et al., 1999). We have selected the median of the estimate for ε_f (26‰) with an uncertainty of 1‰, derived from chemostat culture experiments (e.g., Laws et al., 1995; Popp et al., 1998). The b value represents an integration of all the physiological variables that affect the total carbon isotope fractionation during photosynthesis (e.g., growth rate and cell geometry (Jasper et al., 1994; Bidigare et al., 1997). In this study, the b-value was calculated using the geometric mean regression of all available data (Bidigare et al., 1997, 1999; Eek et al., 1999; Popp et al., 1999; Laws et al., 2001) and mean annual phosphate concentration from the NOAA World Ocean Atlas 2001 (Conkright et al., 2002) for the core-site location (27.5° S).

Values of CO_{2aq} were converted to pCO_2 by applying Henry's Law (Weiss, 1974), calculated assuming an annual mean salinity of 34.6 psu (Conkright et al., 2002) for the core-site (27.5° S), and alkenone-based temperature (Lyle et al., 1992).

The age model was based on seven ^{14}C AMS dates and linear interpolation between the age control points in the upper half of the core (from 40 to 9 kyr BP) (see Mohtadi and Hebbeln, 2004).

3 Results and discussion

3.1 Sea surface temperature reconstruction and possible oceanographic scenarios

At 27.5° S off Chile, the $U^{K'}_{37}$-SST of core GeoB 3375-1 exhibits a millennial-scale variation of the order of ~4 °C during the last 30 kyr BP (Fig. 1a). The core highlights an overall warming trend from 17 °C to 20 °C between ~30 and 17 kyr BP (Fig. 1a). This warming trend was interrupted by cold-events, at ~27, 23 and 16–17 kyr BP. The latter was a very abrupt cooling of almost 4 °C which was followed by a marked increase in SST during the deglacial. Alkenone-SST and the δ^{18}O-*N. pachyderma (sin.)* records in core GeoB 3375-1 are similar between 30 and 20 kyr BP in terms of general pattern and cold events, and between 15 and 10 kyr BP with respect to the deglacial warming (Fig. 1a, b). They differ markedly in the interval 20–15 kyr BP: the alkenone-SST warming trend (of ~1.5 °C) around 19–17 kyr BP and the large and abrupt 16–17 kyr BP cooling are not seen in the δ^{18}O record. This difference between surface waters (recorded by alkenones which are biosynthesized by some algae of the class *Haptophyceae*; e.g., Prahl et al., 1988) and deeper waters (recorded by *N. pachyderma (sin.)* assumed to calcify at depth below the pycnocline; e.g. Andersson et al., 2009) may point to enhanced stratification of the water column during this time. This was previously proposed by De Pol-Holz et al. (2006) who invoked a collapse of thermocline ventilation due to reduced subduction rates of Eastern South Pacific Intermediate Water (ESPIW) triggered by the melting of the Patagonian Ice Sheet, promoting nitrogen removal that potentially contributed to the changes in atmospheric CO_2 during the deglacial (De Pol-Holz et al., 2007).

The deglacial warming (between ~15 and 10 kyr BP, Fig. 1a and b) indicates substantial changes in subsurface water conditions in the ESP with an increased southward advection of the tropical-sourced subsurface waters, suggesting a reorganization of the system that lags the onset of the initial SST warming recorded in core GeoB3375 (Fig. 1a) and other cores off northern and central Chile (Mohtadi and Hebbeln, 2004). The reorganization included reestablishing upwelling and ventilation, with the consequence of a mixed and CO_2-supersaturated water column (Fig. 1c).

On the other hand, the Last Glacial Maximum (LGM) is not observed in the alkenone-SST and δ^{18}O records. Previous studies suggested that during the coldest events (e.g., LGM), the SST gradients between 30° S and the equator seem to have been relatively weaker due to a stronger Peru-Chile Current (PCC) (e.g., Kaiser et al., 2005). In fact, the northward displacement of the oceanographic fronts during the LGM in the ESP (Kaiser et al., 2005) could have increased the upwelling strength, and also the formation rates of ESPIW and ventilation of the shallow oceanic layer off northern Chile (De Pol-Holz et al., 2006). On this basis, the enhanced upwelling and ventilation during the LGM would be reflected in a CO_2-supersaturated water column (Fig. 1c, see also discussion next section).

3.2 The pathways of sea surface carbon dioxide (pCO_2)

The measured $C_{37:2}$-alkenone $\delta^{13}C$ values ranged from −29.5‰ to −20.5‰, and the resulting isotopic fractionation (ε_p) and sea surface pCO_2 ranged from 5.7‰ to 15.9‰ (Table 1S, data supplement: http://www.clim-past-discuss.net/6/347/2010/cpd-6-347-2010-supplement.pdf) and from 200.7 µatm to 415.7 µatm, respectively, for the timeframe 30 to 10 kyr BP (Fig. 1c). The sea surface pCO_2 showed a notable decoupling with the atmospheric CO_2 record (e.g., Indermühle et al., 2000) during the last glacial and the early deglacial (Fig. 1c and d). The sea surface pCO_2 displayed a gradual increase between ∼30 and 28 kyr BP (from 250 to 350 µatm), followed by a gradual decrease between ∼27 and 24.5 kyr BP (from 346 to 235 µatm). Between 24 and ∼17 kyr BP, while atmospheric CO_2 was relatively low and stable (∼200 ppmv, Fig. 1d), highest sea surface pCO_2 values (350–400 µatm, Fig. 1c) suggest that the water column remained supersaturated-CO_2 until stratified conditions stopped ventilation of the water column (De Pol-Holz et al., 2006). Consequently, the pCO_2 gradually declined and this lasted until ∼14 kyr BP (Fig. 1c). In contrast, atmospheric CO_2 increased steadily from ∼18 kyr BP to the start of the Holocene (Fig. 1d).

In summary, the sea surface pCO_2 exhibited higher levels than atmospheric CO_2, highlighting that the upwelling system off northern Chile (27.5° S) may have been continuously supersaturated with CO_2 (Fig. 1c and d), and thus would have been an uninterrupted source of CO_2 to the atmosphere during the period 30–10 kyr BP.

The sea surface pCO_2 is affected by changes in temperature, salinity, total CO_2 concentration (i.e., dissolved inorganic carbon DIC), and alkalinity. While the water temperature is primarily regulated by physical processes (i.e., solar energy input, sea-air heat exchanges, and mixed-layer thickness), the latter two are primarily controlled by biological processes (i.e., photosynthesis, respiration and calcification) and by upwelling of subsurface waters enriched in respired CO_2 and nutrients (e.g., Zeebe and Wolf-Gladrow, 2001; Anderson et al., 2009).

Given that the changes in the sea surface ocean pCO_2 levels could result in important changes in calcareous and/or organic carbon production rates (due to changes in DIC availability; e.g., Zeebe and Wolf-Gladrow, 2001), we analyzed the potential uptake pathways of marine CO_2 between 30 and 10 kyr BP off northern Chile.

We interpret the record of $\delta^{13}C$ of planktonic foraminifera *N. pachyderma (sin.)* (Fig. 1e) in terms of DIC availability (e.g., Köhler et al., 2005) for carbonaceous organisms instead of using it solely as an upwelling strength proxy, as suggested for this region by Dezileau et al. (2004). The $\delta^{13}C$ of *N. pachyderma (sin.)* record displayed a similar pattern to the carbonate ($CaCO_3$) fluxes (Fig. 1e and f). In general terms, when $\delta^{13}C$ is enriched in ^{13}C, the carbonate rain rate decreases. The relative abundance of *G. bulloides* (Fig. 1g) also exhibited a similar pattern since the LGM and especially since ~15 kyr BP during the reorganization period when the three variables highlight the highest carbonate production, in contrast to the late glacial (Fig. 1e, f and g).

We consider that the glacial increase in organic carbon export as well as biogenic opal fluxes (Fig. 1i and j) occurs under iron-enriched conditions (Fig. 1h). The response of inorganic/organic to the sea surface CO_2 concentrations (Fig. 2) suggests that organic carbon production was favored during this time. On this basis, the iron availability is a critical factor that determines the diatom biological pump as a pathway of carbon (Fig. 1c) to the deeper waters in the form of diatom organic carbon (Fig. 1i and j). In fact, a local experiment developed in the coastal upwelling areas off Chile evidenced that diatom growth and their capacity to lower the high-pCO_2 of recently-upwelled waters, depend on additional inputs of iron (Torres and Ampuero, 2009).

A large reduction in pCO_2 occurred between ~27 and 24 kyr BP, during the gradual iron-enrichment of the water column, which might be related to the pronounced increase of total organic carbon and biogenic opal fluxes (Fig. 1i and j), suggesting that iron enhanced the capacity of the phytoplankton community, probably dominated by diatoms, to rapidly lower the $p\mathrm{CO}_2$ surface levels, activating a strong biological pump able to rapidly reduce the intense CO_2 outgassing. Furthermore, the impoverishment in ^{13}C of the δ^{13}C-*N. pachyderma (sin.)* (Fig. 1e), indicates high-DIC availability, which was destined mainly to the photosynthesis process. Moreover, the response of inorganic/organic carbon to CO_2 concentration (Fig. 2) describes that whereas CO_2 dissolution decreases in the sea surface waters, the organic carbon production remained above carbonate production.

Between ~24 and 17 kyr BP the water column remained highly supersaturated in CO_2 without significant depletion, due to more $p\mathrm{CO}_2$ released to the atmosphere through the upwelling process. During this period, the high-export of iron-rich terrigenous material (Dezileau et al., 2004) permitted an increase of the total productivity, reflected in the high-organic carbon (Fig. 1i), -biogenic opal (Fig. 1j) and -carbonate (Fig. 1f) fluxes. However, the high-total production in the water column was not enough to counteract the high-concentrations of dissolved CO_2 in the water.

During the deglacial warming (~17–16 kyr BP, see gray hachured bar in Fig. 1), the well-stratified water column and the collapse of the ESPIW formation (De Pol-Holz et al., 2006) apparently favored the decrease in $p\mathrm{CO}_2$ (Fig. 1c). We expected that surface stratification not only would help maintain primary producers close to the surface (by limiting the depth of turbulent mixing) but also isolate the mixed layer from CO_2-rich and nutrients-rich water located below the pycnocline. In fact, a slight reduction in organic carbon and opal fluxes is also observed during this period (Fig. 1i and j). On the other hand, all productivity proxies for calcareous organisms displayed a slight increase during this period (Fig. 1f–g), probably favoring a reduction in water column DIC (Fig. 1e).

A simultaneous intensification of the upwelling in the Southern Ocean (SO) would explain the deglacial rise in the atmospheric CO_2 (Fig. 1d) and the high-inputs of nutrients to the SO (Anderson et al., 2009). We would expect that the intense upwelling and high-opal fluxes recorded in the ~16–10 kyr BP period in the SO (Anderson et al., 2009), would lead to the formation of particularly macro-nutrient rich waters (specifically the

Subantarctic Mode Water, SAMW). However, the strong-iron limitation associated to deep upwelled waters implies that the waters formed in this period were impoverished in iron and silicates, but enriched in nitrate (Anderson et al., 2009). Therefore, a tendency to develop a secondary silicate limitation (Hutchins and Brunland, 1998; Takeda, 1998; Martin-Jézéquel et al., 2000) while still retaining high-nitrate (Sarmiento et al., 2007). Thus, the upwelling of SAMW (originally formed from upper Circumpolar Deep Water) by wind driven upwelling systems is expected to lead silicate limitation, and consequently non-siliceous functional groups dominated the phytoplankton assemblage during this period, increasing their influence in the biological pump. This scenario is supported by the decoupling recorded between organic carbon (Fig. 1i), total nitrogen (Fig. 1j) and opal fluxes (Fig. 1j), during ∼16–10 kyr BP. Certainly, the maximum export of organic carbon during this period (∼16–10 kyr BP) corresponds to both a maximum of $CaCO_3$ (Fig. 1f) and minimum of opal fluxes (Fig. 1j).

The contrast between the trends of biogenic opal and organic carbon fluxes between ∼16 and 10 kyr BP off northern Chile could be reconciled by invoking a shift in the phytoplankton communities from diatomaceous to carbonate production. This would have reduced and increased relative contributions of organic carbon and carbonate to total export production, respectively (Fig. 1i and j).

The apparent contrast (i.e., late glacial/deglacial) becomes clear if we consider how the decrease in terrigenous iron inputs (Fig. 1h) affected the nitrate, as well as silicic acid utilization by diatoms, reducing the total nitrogen and opal fluxes (Fig. 1j), and consequently their role in the marine CO_2 drawdown by the biological pump (Fig. 1i).

High-carbonate drawdown (Fig. 1f and g) at warm-SST (Fig. 1a) and high-atmospheric CO_2 (Fig. 1d), suggest that the marine DIC was captured intensively by the carbonate system, enhancing the carbonate precipitation of the calcifying organisms in the plankton assemblage (Fig. 2). On basis of experimental results from Iglesias-Rodriguez et al. (2008), probably, the deglacial rise of the atmospheric CO_2 could also increase calcification rates, and its drawdown to the deep-ocean through the pathway of the carbonate system (Fig. 1f). In fact, the light-δ^{13}C of *N. pachyderma* *(sin.)* signal (Fig. 1e) confirms this hypothesis, since the elevated impoverishment in ^{13}C could be indicative of a major and rapid consumption of DIC by calcifying organisms.

The calcification increment reduces the efficiency of the marine ecosystem to store sea surface CO_2, due to changes in the buffering capacity of the ocean's carbonate system, as well as to draw down the atmospheric CO_2 (Cermeño et al., 2008). In fact, if (1) calcium carbonate precipitation increases the marine pCO$_2$ (e.g., Zeebe and Wolf-Gladrow, 2001) and (2) a high-pCO$_2$ increases the calcification rates (e.g. Iglesias-Rodriguez et al., 2008), a positive feedback will tend to increase the calcification processes. On this basis, only biologically active iron-enrichment conditions would enhance the competitive advantages of diatoms to break the positive feedback and shift the system to capture the marine CO_2 pathway biological pump.

Our findings suggest that the coastal ocean off northern Chile has been a permanent and strong source of CO_2 to the atmosphere between 30 and 10 kyr BP. This CO_2 outgassing has been modulated by local (upwelling strength) and global mechanisms (e.g., ocean circulation, atmospheric CO_2) that have changed the water column properties (e.g., water column stability, macro- and micro-nutrients availability), and consequently driven the role and importance of the biological pump and the marine carbonate system in the sequestration of inorganic carbon to the deep-ocean.

4 Concluding remarks

The sea surface pCO$_2$ reconstruction indicates that the coastal ocean off northern Chile (~27.5° S) has been a permanent and strong upwelling source of CO_2 to the atmosphere between 30 and 10 kyr BP. The multiproxy reconstruction reveals that the CO_2 outgassing and sequestration was modulated by local and global mechanisms. During the global glacial period, the water column remained highly supersaturated in CO_2, due to more pCO$_2$ being released to the atmosphere through upwelling process. Furthermore, the fertilization of iron biologically active and macronutrients intensified the carbon sequestration pathway biological pump through diatom biomass export. In contrast, during the deglacial warming the iron-limitation altered significantly the marine CO_2 sequestration pathway biological pump. Warm-SST and high-atmospheric CO_2 conditions suggest that the carbon was captured intensively by the carbonate system, enhancing the carbonate precipitation of the calcifying organisms in the plankton assemblage. Overall findings suggest that biologically active iron-availability conditions controlled the competitive advantages of plankton to shift the system to capture the marine CO_2 pathway biological pump and/or carbonate system off northern Chile in the eastern south Pacific margin between 30 and 10 kyr BP.

Acknowledgements. We thank to M. Sato (JAMSTEC) for her valuable help with alkenone analyses. This work was funded by the JAMSTEC Institution and the FONDAP-COPAS Center (Grant No. 150100007). J.A. Placencia was supported by scholarships granted by the Ministry of Education-Chile (Grant MECESUP/UCO-0002), the Graduate School at University of Concepcion, and by the POGO-IOC-SCOR fellowship 2005.

References

Anderson, R. F., Ali, S., Bradtmiller, L. I., Nielsen, S. H. H., Fleisher, M. Q., Anderson, B. E., and Burckle, L. H.: Wind-driven upwelling in the Southern Ocean and the deglacial rise in atmospheric CO_2, Science, 323, 1443–1448, 2009.

Andersson, C., Pausata, F. S. R., Jansen, E., Risebrobakken, B., and Telford, R. J.: Holocene trends in the foraminifer record from the Norwegian Sea and the North Atlantic Ocean, Clim. Past Discuss., 5, 2081–2113, 2009, http://www.clim-past-discuss.net/5/2081/2009/.

Bakker, D., Watson, A., and Law, C.: Southern Ocean iron enrichment promotes inorganic carbon drawdown, Deep-Sea Res. II, 48, 2483–2507, 2001.

Bidigare, R. R., Fluegge, A., Freeman, K. H., Hanson, K. L., Hayes, J. M., Hollander, D., Jasper, J. P., King, L. L., Laws, E. A., Milder, J., Millero, F. J., Pancost, R., Popp, B. N., Steinberg, P. A., and Wakeham, S. G.: Consistent fractionation of ^{13}C in nature and in the laboratory: Growth rate in some haptophyte algae, Global Biogeochem. Cycles, 11, 279–292, 1997.

Bidigare, R. R., Hanson, K. L., Buesseler, K., Wakeham, S. G., Freeman, K. H., Pancost, R. D., Millero, F. J., Steinberg, P., Popp, B. N., Latasa, M., Landry, M. R., and Laws, E. A.: Iron-stimulated changes in ^{13}C fractionation and export by equatorial Pacific phytoplankton: Toward a paleo-growth rate proxy, Paleoceanography, 14, 589–595, 1999.

Borges, A. V., Delille, B., and Frankignoulle, M.: Budgeting sinks and sources of CO_2 in the coastal ocean: diversity of ecosystems counts, Geophys. Res. Lett., 32, L14601, doi:10.1029/2005GL023053, 2005.

Bruland, K. W., Rue, E. L., Smith, G. J., and DiTullio, G. R.: Iron, macronutrients and diatom blooms in the Peru upwelling regime: brown and blue waters of Peru, Mar. Chem., 93, 81–103, 2005.

Cermeño, P., Dutkiewicz, S., Harris, R. P., Follows, M., Schofield, O., and Falkowski, P. G.: The role of nutricline depth in regulating the ocean carbon cycle, Proc. Natl. Acad. Sci. USA, 105, 20344–20349, 2008.

Conkright, M. E., Locarnini, R. A., Garcia, H. E., O'Brien, T. D., Boyer, T. P., Stephens, C., and Antonov, J. I.: World Ocean Atlas 2001: Objective Analyses, Data Statistics, and Figures, CD-ROM Documentation. National Oceanographic Data Center, Silver Spring, MD, 17 pp., 2002.

Dezileau, L., Ulloa, O., Hebbeln, D., Lamy, F., Reyss, J., and Fontugne, M.: Iron control of past productivity in the coastal upwelling system off the Atacama Desert, Chile, Paleoceanography, 19, PA3012, doi:10.1029/2004PA001006, 2004.

de Baar, H. J. W. and Boyd P. M.: The role of iron in plankton ecology and carbon dioxide transfer of the global oceans, in: The Dynamic Ocean Carbon Cycle: A Midterm Synthesis of the Joint Global Ocean Flux Study, edited by: Hanson R. B., Ducklow, H. W., and Field, J. G., International Geosphere Biosphere Programme Book Series vol. 5, Cambridge University Press, Cambridge, pp. 61–140, 2000.

De Pol-Holz, R., Ulloa, O., Dezileau, L., Kaiser, J., Lamy, F., and Hebbeln, D.: Melting of Patagonian ice sheet and deglacial perturbations of the nitrogen cycle in the eastern South Pacific, Geophys. Res. Lett., 33, L04704, doi:10.1029/2005GL024477, 2006.

De Pol-Holz, R., Ulloa, O., Lamy, F., Dezileau, L., Sabatier, P., and Hebbeln, D.: Late Quaternary variability of sedimentary nitrogen isotopes in the eastern South Pacific Ocean, Paleoceanography, 22, PA2207, doi:10.1029/2006PA001308, 2007.

Eek, M. E., Whiticar, M. J., Bishops, J. K. B., and Wong, C. S.: Influence of nutrients on carbon isotope fractionation by natural populations of Pymnesiophyte algae in NE Pacific, Deep Sea

Res. II, 46, 2863–2876, 1999.

Freeman, K. H. and Pagani, M.: Alkenone-based estimates of past CO_2 levels: a consideration of their utility based on an analysis of uncertainties, in: A History of Atmospheric CO_2 and its Effects on Plants, edited by: Ehleringer, J. R., Cerling, T. E., and Dearing, M. D., Animals, and Ecosystems, Ecological Studies, Springer, New York, pp. 35–60, 2005.

Friederich, G. E., Ledesma, J., Ulloa, O., and Chavez, F. P.: Air–sea carbon dioxide fluxes in the coastal southeastern tropical Pacific, Prog. Oceanogr., 79, 156–166, 2008.

Gonzalez-Mora, B., Sierro, F. J., and Flores, J. A.: Controls of shell calcification in planktonic foraminifers, Quat. Sci. Rev., 27, 956–961, 2008.

Harada, M., Shin, K. H., Murata, A., Uchida, M., and Nakatani, T.: Characteristics of alkenones synthesized by a bloom of Emiliania huxleyi in the Bering Sea, Geochim. Cosmochim. Acta, 67, 1507–1519, 2003.

Hebbeln, D., Marchant, M., and Wefer, G.: Seasonal variations of the particle flux in the Peru-Chile current at 30° S under 'normal' and El Niño conditions, Deep-Sea Res. II, 47, 2101–2128, 2000.

Hutchins, D. A. and Bruland, K. W.: Iron-limited diatom growth and Si:N ratios in a coastal upwelling regime, Nature, 393, 561–564, 1998.

Iglesias-Rodriguez, M. D., Halloran, P. R., Rickaby, R. E. M., Hall, I. R., Colmenero-Hidalgo, E., Gittins, J. R., Green, D. R. H., Tyrrell, T., Gibbs, S. J., von Dassow, P., Rehm, E., Armbrust, E. V., and Boessenkool, K. P.: Phytoplankton calcification in a high-CO_2 World, Science, 320, 336–340, 2008.

Indermühle, A., Monnin, E., Stauffer, B., Stocker, T. F., and Wahlen, M.: Atmospheric CO_2 concentration from 60 to 20 kyr BP from the Taylor Dome ice core, Antarctica, Geophys. Res. Lett., 27, 735–738, 2000

Jasper, J. P., Mix, A. C., Prahl, F. G., and Hayes, J. M.: Photosynthetic fractionation of ^{13}C and concentrations of dissolved CO_2 in the central equatorial Pacific during the last 255,000 years, Paleoceanography, 6, 781–798, 1994.

Johnson, K. S., Chavez, F. P., and Friederich, G. E.: Continental shelf sediment as a primary source of iron for coastal phytoplankton, Nature, 398, 697–700, 1999.

Kaiser, J., Lamy, F., and Hebbeln, D.: A 70-kyr sea surface temperature record off southern Chile (ODP Site 1233), Paleoceanography, 20, PA4009, doi:10.1029/2005PA001146, 2005.

Köhler, P., Fischer, H., Munhoven, G., and Zeebe, R. E.: Quantitative interpretation of atmospheric carbon records over the last glacial termination, Global Biogeochem. Cycles, 19, GB4020, doi:10.1029/2004GB002345, 2005.

Lamy, F., Kaiser, J., Ninnemann, U., Hebbeln, D., Arz, H. W., and Stoner, J.: Antarctic timing of surface water changes off Chile and Patagonian ice sheet response, Science, 304, 1959–1962, 2004.

Laws, E. A., Popp, B. N., Bidigare, R. R., Kennicut, M. C., and Macko, S. A.: Dependence of phytoplankton carbon isotopic composition on growth rate and $[CO_2]_{aq}$: theoretical considerations and experimental results, Geochim. Cosmochim. Acta, 59, 1131–1138, 1995.

Laws, E. A., Popp, B. N., Bidigare, R. R., Riebesell, U., Burkhardt, S., and Wakeham, S. G.: Control on the molecular distribution and carbon isotopic composition of alkenones in certain haptophyte algae, Geochem. Geophys. Geosyst., 2, paper number 2000GC000057, 2001.

Lyle, M., Zahn, R., Prahl, F., Dymond, J., Collier, R., Pisias, N., and Suess, E.: Paleoproductivity and carbon burial across the California Current: the Multitracers Transect, 42° N, Paleoceanography, 7, 251–272, 1992.

Marchant, M., Hebbeln, D., Giglio, S., Coloma, C., and González, H.: Seasonal and interannual variability in the flux of planktic foraminifera in the Humboldt Current System off central Chile (30° S), Deep-Sea Res. II, 51, 2441–2455, 2004.

Martin, J.: Glacial–interglacial CO_2 change: the iron hypothesis, Paleoceanography, 5, 1–13, 1990.

Martin-Jézéquel, V., Hildebrand, M., and Brzezinski, M. A.: Silicon metabolism in diatoms: implications for growth, J. Phycol., 36, 821–840, 2000.

Mohtadi, M. and Hebbeln, D.: Mechanisms and variations of the paleoproductivity off northern Chile (24° S–33° S) during the last 40,000 years, Paleoceanography, 19, PA2023, doi:10.1029/2004PA001003, 2004.

Mohtadi, M., Hebbeln, D., and Marchant, M.: Upwelling and productivity along the Peru–Chile Current derived from faunal and isotopic compositions of planktic foraminifera in surface sediments, Mar. Geol., 216, 107–126, 2005.

Mohtadi, M., Rossel, P., Lange, C. B., Pantoja, S., Böning, P., Repeta, D. J., Grunwald, M., Lamy, F., Hebbeln, D., and Brumsack, H.: Deglacial pattern of circulation and marine productivity in the upwelling region off central-south Chile, Earth Planet. Sci. Lett., 272, 221–230, 2008.

Pagani, M., Arthur, M. A., and Freeman, K. H.: Miocene evolution of atmospheric carbon dioxide, Paleoceanography, 14, 273–292, 1999.

Paulmier, A., Ruiz-Pino, D., and Garcon, V.: The oxygen minimum zone(OMZ) off Chile as intense source of CO_2 and N_2O, Con. Shelf Res., 28, 2746–2756, 2008.

Popp, B. N., Laws, E. A., Bidigare, R. R., Dore, J. E., Hanson, K. L., and Wakeham, S. G.: Effect of phytoplankton cell geometry on carbon isotopic fractionation, Geochim. Cosmochim. Acta, 62, 69–77, 1998.

Popp, B. N., Hanson, K. L., Dore, J. E., Bidigare, R. R., Laws, E. A., and Wakeham, S. G.: Controls on the carbon isotopic composition of phytoplankton: paleoceanographic perpectives, in: Reconstructing ocean history: a window into the future, edited by: Abrantes, F. and Mix, A., New York: Plenum, pp. 381–398, 1999.

Prahl, F. G., Muehlhausen, L. A., and Zahnle, D.: Further evaluation of long-chain alkenones as indicators of paleoceanographic conditions, Geochim. Cosmochim. Acta, 52, 2303–2310, 1988.

Prahl, F. G. and Wakeham, S. G.: Calibration of unsaturation patterns in long-chain ketone compositions for paleotemperature assessment, Nature, 330, 367–369, 1987.

Sarmiento, J. L., Simeon, J., Gnanadesikan, A., Gruber, N., Key, R. M., and Schlitzer, R.: Deep ocean biogeochemistry of silicic acid and nitrate, Global Biochem. Cycles, 21, GB1S90, doi:10.1029/2006GB002720, 2007.

Shaffer, G., Hormazabal, S., Pizarro, O., and Salinas, S.: Seasonal and interannual variability of currents and temperature off central Chile, J. Geophys. Res., 104, 29951–29961, 1999.

Simpson, J. J. and Zirino, A.: Biological control of pH in the Peruvian coastal upwelling area, Deep-Sea Res., 27, 733–744, 1980.

Smith, H. J., Fischer, H., Mastroianni, D., Deck, B., and Wahlen, M.: Dual modes of the carbon cycle since the Last Glacial Maximum, Nature, 400, 248–250, 1999.

Takeda, S.: Influence of iron availability on nutrient consumption ratio of diatoms in oceanic waters, Nature, 393, 774–777, 1998.

Torres, R., Turner, D. R., Silva, N., and Rutllant, J.: High short-term variability of CO_2 fluxes during an upwelling event off the Chilean coast at 30° S, Deep-Sea Res. I, 46, 1161–1179, 1999.

Torres, R. and Ampuero, P.: Strong CO_2 outgassing from high nutrient low chlorophyll coastal waters off central Chile (30° S): The role of dissolved iron, Estuar. Coast. Shelf Sci., 83, 126–132, 2009.

Torres, R., Turner, D. R., Rutllant, J., Sobarzo, M., Antezana, T., and Gonzalez, H.: CO_2 outgassing off central Chile (31–30° S) and northern Chile (24–23° S) during austral summer 1997: The effect of wind intensity on the upwelling and ventilation of CO_2-rich waters, Deep

Sea Res., Part I, 49, 1413–1429, 2002.
Zeebe, R. E. and Wolf-Gladrow, D.: CO_2 in Seawater: Equilibrium, Kinetics, Isotopes, Elsevier Oceanography Series, 65, pp. 346, 2001.

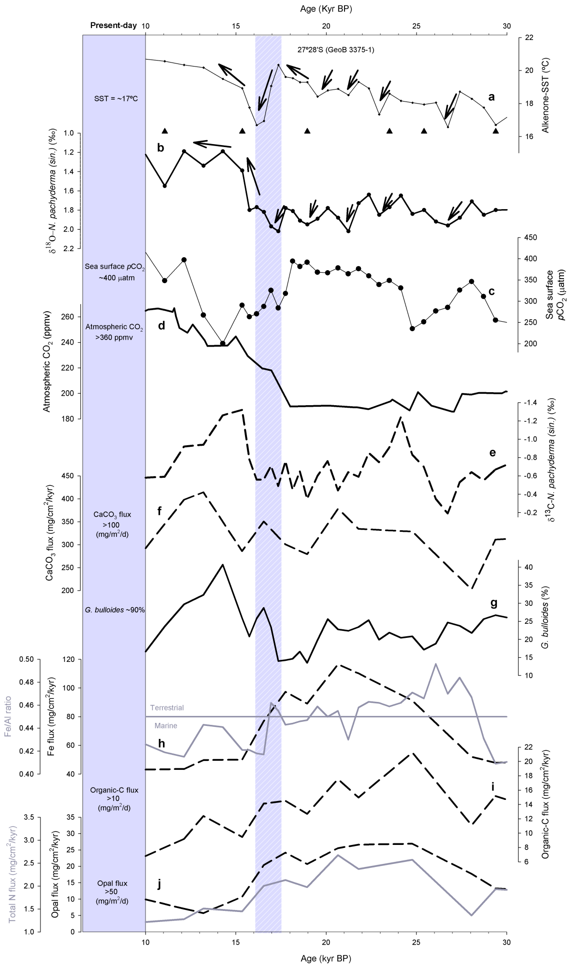
Age (Kyr BP)
Present-day
10
15
20
25
30
27°28'S (GeoB 3375-1)
SST = ~17°C
a
Alkenone-SST (°C)
22
20
18
16
δ^{18}O–N. pachyderma (sin.) (‰)
1.0
1.2
1.4
1.6
1.8
2.0
2.2
b
Sea surface pCO$_2$ ~400 μatm
Sea surface pCO$_2$ (μatm)
450
400
350
300
250
200
c
Atmospheric CO$_2$ >360 ppmv
Atmospheric CO$_2$ (ppmv)
260
240
220
200
180
d
δ^{13}C–N. pachyderma (sin.) (‰)
-1.4
-1.2
-1.0
-0.8
-0.6
-0.4
-0.2
e
CaCO$_3$ flux >100 (mg/m^2/d)
CaCO$_3$ flux (mg/cm^2/kyr)
450
400
350
300
250
200
f
G. bulloides ~90%
G. bulloides (%)
40
35
30
25
20
15
10
g
Fe/Al ratio
0.50
0.48
0.46
0.44
0.42
0.40
Fe flux (mg/cm^2/kyr)
120
100
80
60
40
Terrestrial
Marine
h
Organic-C flux >10 (mg/m^2/d)
Organic-C flux (mg/cm^2/kyr)
22
20
18
16
14
12
10
8
6
i
Total N flux (mg/cm^2/kyr)
3.5
3.0
2.5
2.0
1.5
1.0
Opal flux (mg/cm^2/kyr)
35
30
25
20
15
10
5
0
Opal flux >50 (mg/m^2/d)
j
Age (kyr BP)

Fig. 1.

Fig. 1. Core GeoB3375-1 off northern Chile. A multiproxy reconstruction between 30 and 10 kyr BP: **(a)** Alkenone-based SST (this study). **(b)** $\delta^{18}O$ of *N. pachyderma (sin)* (Dezileau et al., 2004). **(c)** Sea surface $p\mathrm{CO}_2$ (this study). **(d)** Atmospheric CO_2 concentration in the Antarctic Taylor Dome ice core (composite data from Smith et al., 1999, and Indermühle et al., 2000). **(e)** $\delta^{13}C$ of *N. pachyderma (sin)* (Dezileau et al., 2004). **(f)** *$CaCO_3$ fluxes. **(g)** The relative abundance of *G. bulloides* (Mohtadi and Hebbeln, 2004). **(h)** *Iron fluxes (black doted line) and the Fe/Al ratio (gray line). The Fe/Al ratio indicates marine vs. terrigenous sources of iron (Dezileau et al., 2004). **(i)** *Organic carbon fluxes. **(j)** *Biogenic Opal and *Total Nitrogen fluxes. Gray hatched bar indicates the onset of increased stratification off 30° S (De Pol-Holz et al., 2006). Gray solid bar on left-hand side represents present-time values (Table 2S, data supplement: http://www.clim-past-discuss.net/6/347/2010/cpd-6-347-2010-supplement.pdf). *Thorium-230 normalized fluxes (see details in Dezileau et al., 2004).

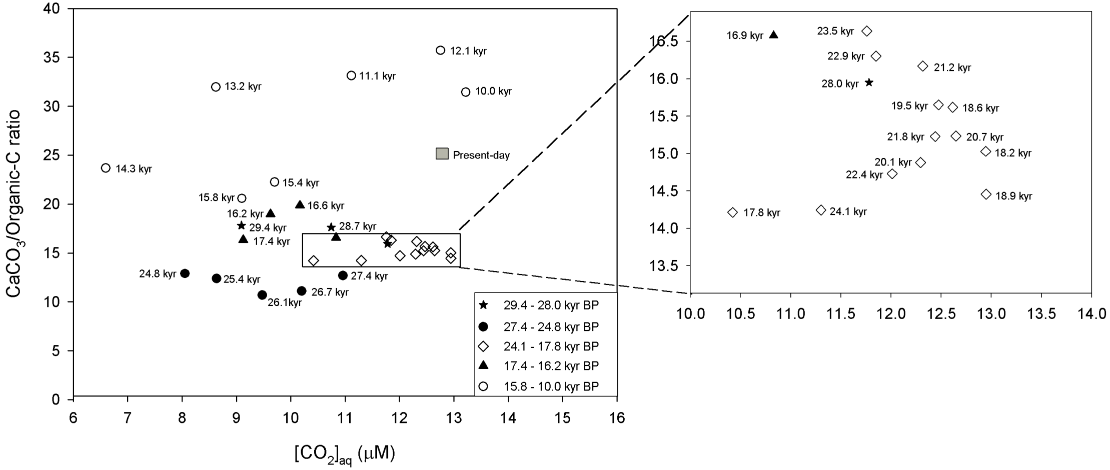

Fig. 2. Response of inorganic ($CaCO_3$) and organic Carbon (Organic-C) to the CO_2 concentration in sea surface waters between 10 and 30 kyr BP. Time intervals were delimited according to sea surface pCO_2 changes (Fig. 1c). Gray solid square represents the present-day relationship between the $CaCO_3$/organic-C ratio and CO_2 concentration in sea surface waters at the study site (Table 2S: http://www.clim-past-discuss.net/6/347/2010/cpd-6-347-2010-supplement.pdf).